RSC Advances

ROYAL SOCIETY OF CHEMISTRY

www.rsc.org/advances

Journal Name

RSCPublishing

ARTICLE

Transition metal induced switch of fluorescence and absorption response of Zn(II)porphyrin-DNA conjugate to cysteine derivatives

Cite this: DOI: 10.1039/x0xx00000x

Received 00th January 2012,
Accepted 00th January 2012

DOI: 10.1039/x0xx00000x

www.rsc.org/

Jung Kyu Choi,[a] Gevorg Sargsyan,[a] Breiana D. Johnson[a] and Milan Balaz*[a]

We report a supramolecular zinc(II)tettraarylporphyrin-oligothymidine/metal ion system (**ZnPorT8**/M^{2+}) for dual optical sensing of cysteine (Cys) and glutathione (GSH) with tunable spectroscopic outcome. Transition metal ions (M^{2+} = Hg^{2+} or Cu^{2+}) allow to switch the emission and absorption response of the **ZnPorT8**/M^{2+} complex. The **ZnPorT8**/Hg^{2+} complex exhibits turn-on fluorescence sensing (fluorescence enhancement), while the **ZnPorT8**/Cu^{2+} system exhibits turn-off sensing (emission quenching) of Cys and GSH. The **ZnPorT8**/Hg^{2+} and **ZnPorT8**/Cu^{2+} complexes have excellent limit of detection (LOD_{em}) for Cys (5.95 nM and 11.99 nM, respectively) and GSH (3.34 nm and 13.50 nM, respectively).

Introduction

Porphyrins and metalloporphyrins have found widespread use as recognition and/or reporting components in many diverse sensing systems due to their modular electronic and structural properties.[1-6] They have been successfully used for fluorescence mapping of viscosity,[7, 8] electrochemical detection of explosives,[9] chiroptical sensing of left-handed Z-DNA,[10-13] phosphorescent oxygen sensing,[14] emission detection of Cu(II),[15] amperometric sensing of organophosphate pesticides,[16] or optical determination of bacterial exosporium sugars.[17] We have recently reported highly sensitive optical detection of Hg^{2+} by the zinc(II)porphyrin-oligothymidine bioconjugate **ZnPorT8** (Figure 1).[18] The addition of Hg(II) and Cu(II) lead to complete and partial emission quenching, respectively. The quenching was very likely caused by photoinduced electron transfer upon binding of mercury(II) to trispyridylphenyl-porphyrin. Mercury and copper ions exhibit very high affinity for thiol group and form stable complexes with cysteine.[19, 20] Interaction between Cys and Hg(II) has been utilized for turn-on[21-28] or turn-off[29, 30] emission sensing of Cys by multicomponent supramolecular systems with excellent detection limits ranging from 2.0 to 600 nM. Similarly, Cu-complexes have been explored for spectrophotometric Cys detection.[31-34] Detection of Cys and its derivative glutathione (GSH) is of high importance for diagnosing biothiol related health problems[35-39], since Cys and GSH are crucial in maintaining the physiological redox homeostasis in biological systems.[40-44] Optical sensing (e.g. fluorescence and absorption) is especially attractive since it is non-destructive, inexpensive, and allows high throughput real time detection without a need for derivatization.[45-47] Herein we report a supramolecular system assembled of **ZnPorT8** and a transition metal ion (either Hg(II) or Cu(II)) for highly sensitive and selective optical sensing of Cys and GSH in water. Importantly, transition metal ions allow switching the emission and absorption recognition response of the **ZnPorT8**/metal complex. The **ZnPorT8**/Hg^{2+} complex offers a turn-on fluorescence sensing (fluorescence enhancement), while the **ZnPorT8**/Cu^{2+} system gives reversed turn-off sensing (emission quenching) of biothiols.

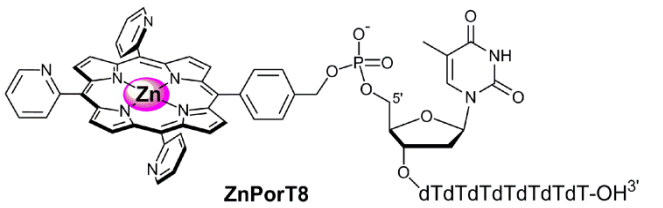

Figure 1. Structure of Zn(II)tetraarylporphyrin-octathymine conjugate **ZnPorT8**.

Results and discussion

ZnPorT8/Hg^{2+} system: Cys and GSH optical sensing

We have shown that the fluorescence of **ZnPorT8** could be significantly decreased (up to 94.2% signal reduction) by Hg^{2+} ions upon their binding to trispyridylphenyl-porphyrin. Since Hg^{2+} ion also forms highly stable complexes with cysteine,[48] we have decided to explore biothiols optical recognition with supramolecular **ZnPorT8**/Hg^{2+} complex. The UV-vis absorption spectrum of a mixture of **ZnPorT8** (2μM) and Hg^{2+} (5.0 μM) in sodium cacodylate buffer (1.0 mM, pH 7.0) showed absorption bands at 428.6 nm (Soret band) and 558.8 nm (Q-

band). The fluorescence spectrum of the **ZnPorT8**/Hg^{2+} system displayed two maxima at 604.0 nm and 654.0 nm when excited at 425.0 nm.[18] Addition of L-Cys (5.0 μM) to the solution of **ZnPorT8**/Hg^{2+} complex ([**ZnPorT8**] = 2.0 μM, [Hg^{2+}] = 5.0 μM) caused a blue shift of the Soret band from 428.6 nm to 425.0 nm together with small hyperchromicity (Figure 2a, red curve). The fluorescence intensity of the **ZnPorT8**/Hg^{2+} complex at 654 nm (λ_{exc} = 425.0 nm) increased 6.21-fold from 130 a.u. to 810 a.u. upon the addition of L-Cys (5.0 μM; Figure 2b, red curve). No cysteine induced shift of the emission maximum of **ZnPorT8**/Hg^{2+} complex was detected. Addition of L-Cys caused the release of the Hg^{2+} from its complex with **ZnPorT8** and formation of a 1:1 L-Cys:Hg^{2+} complex.[48, 49] Addition of D-Cys to **ZnPorT8**/Hg^{2+} system caused virtually identical spectroscopic changes as L-Cys and no chiral discrimination by **ZnPorT8**/Hg^{2+} system was observed (Figure S6). Interaction of GSH with **ZnPorT8**/Hg^{2+} complex promoted very similar spectroscopic changes as did Cys. Addition of GSH (5.0 μM) to the **ZnPorT8**/Hg^{2+} complex ([**ZnPorT8**] = 2.0 μM, [Hg^{2+}] = 5.0 μM) caused a blue shift of the Soret band maximum from 428.6 nm to 424.8 nm accompanied by weak hyperchromicity in the UV-vis absorption spectrum (Figure 2a, blue curve). The emission signal at 654 nm (λ_{exc} = 425.0 nm) increased without any observable λ_{em} shift 6.35-fold from 130 a.u. to 829 a.u. upon addition of GSH (5.0 μM; Figure 2b, blue curve). Addition of GSH caused the dissociation of the **ZnPorT8**/Hg^{2+} and formation of a GSH:Hg^{2+} complex with 3:2 stoichiometry.[48] Addition of L-Cys (5.0 μM) or GSH (5.0 μM) to the solution of **ZnPorT8** (2 μM) in the absence of Hg^{2+} did not cause detectable changes in the UV-vis absorption nor fluorescence spectra of the **ZnPorT8** conjugate (Figures S1-S2).

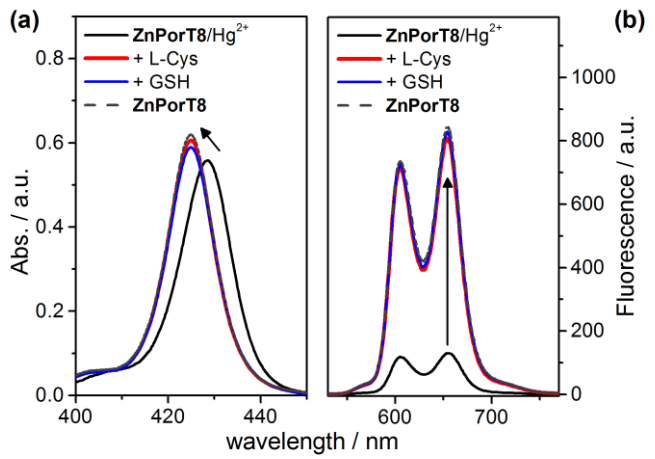

Figure 2. (a) UV-vis absorption and (b) fluorescence spectra of the **ZnPorT8** (2 μM, black dashed lines), **ZnPorT8**/Hg^{2+} complex ([**ZnPorT8**] = 2.0 μM, [Hg^{2+}] = 5.0 μM, black solid lines), **ZnPorT8**/Hg^{2+} in the presence of L-Cys (5.0 μM, red solid lines), and **ZnPorT8**/Hg^{2+} in the presence of GSH (5.0 μM, blue solid lines). Conditions: Na-cacodylate buffer (1.0 mM, pH = 7.0), λ_{exc} = 425 nm. Arrows depict the biothiol induced changes of the **ZnPorT8**/Hg^{2+} spectroscopic signal.

Absorption and emission spectral changes observed upon the addition of Cys or GSH to the **ZnPorT8**/Hg^{2+} complex are strong evidence of binding of biothiols to the Hg^{2+} ions of the **ZnPorT8**/Hg^{2+} complex *via* the thiol functional group.[48] Higher affinity of cysteine for Hg(II) than **ZnPorT8** for Hg(II) caused the **ZnPorT8**/Hg^{2+} complex to fall apart thus releasing the strongly fluorescent **ZnPorT8** conjugate. The comparison of spectroscopic characteristics of **ZnPorT8**/Hg^{2+} complex treated with biothiols (Figure 2, red and blue curves) and **ZnPorT8** conjugate (Figure 2, black dashed lines) has provided final proof that additions of Cys and GSH released **ZnPorT8** from its **ZnPorT8**/Hg^{2+} complex.

ZnPorT8/Cu^{2+} system: Cys and GSH optical sensing

The fluorescence of **ZnPorT8** can also be quenched by Cu^{2+} ions, though less efficiently than with Hg^{2+}. We have therefore explored the biomolecular detection of L-Cys and GSH by the **ZnPorT8**/Cu^{2+} supramolecular system. Figure 3 shows the L-Cys-induced changes in absorption and fluorescence spectra of the **ZnPorT8**/Cu^{2+} system ([**ZnPorT8**] = 2.0 μM, [Cu^{2+}] = 20.0 μM). Addition of L-Cys (6.0 μM) to the solution of **ZnPorT8**/Cu^{2+} complex ([**ZnPorT8**] = 2.0 μM, [Cu^{2+}] = 20.0 μM) caused intense hypochromicity of the Soret band (65%), a red shift of the Soret band maximum from 425.8 nm to 428.6 nm (+2.8 nm; Figure 3a, red curve) and appearance of a shoulder. Addition of Cys (6.0 μM; Figure 3b, red curve) to **ZnPorT8**/Cu^{2+} complex induced fluorescence quenching as evidenced by the decrease of the emission intensity of the **ZnPorT8**/Cu^{2+} complex at 653 nm (λ_{exc} = 426.0 nm) by 87.7% from 653 a.u. to 80 a.u.

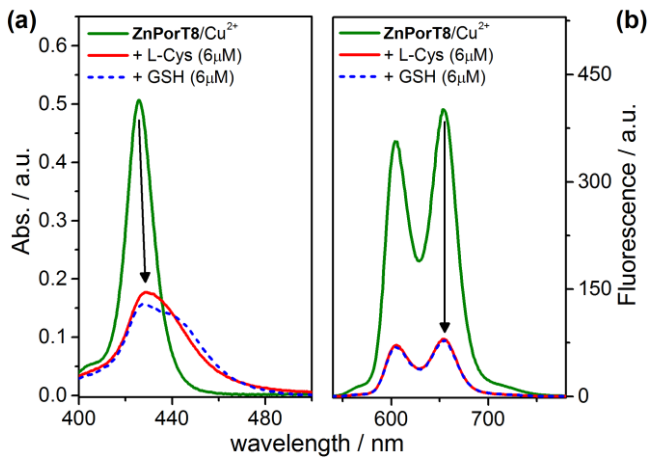

Figure 3. (a) UV-vis absorption and (b) fluorescence spectra of the **ZnPorT8**/Cu^{2+} complex ([**ZnPorT8**] = 2.0 μM, [Cu^{2+}] = 20.0 μM) in the absence of L-Cys (green curves) and in the presence of L-Cys ([L-Cys] = 6.0 μM; red curves). Conditions: Na-cacodylate buffer (1.0 mM, pH = 7.0), λ_{exc} = 426 nm. Arrows depict the biothiol induced changes of the **ZnPorT8**/Cu^{2+} spectroscopic signal.

Similar absorption and emission spectroscopic responses were observed upon addition of GSH (6 μM) to **ZnPorT8**/Cu^{2+} system (Figure 3, blue dashed curves). Changes in absorption and emission spectra observed upon addition of Cys or GSH to the **ZnPorT8**/Cu^{2+} complex confirmed Cys and GSH interactions with Cu^{2+} in **ZnPorT8**/Cu^{2+} complex. Based on literature precedence,[19, 50-52] we hypothesize that Cys and GSH

partially reduced Cu(II) to Cu(I) with Cu(I) complex being a better quencher of **ZnPorT8** emission than Cu(II).

It is important to emphasize that while the addition of L-Cys and GSH caused an enhancement of emission signal of the **ZnPorT8**/Hg^{2+} system, their addition to **ZnPorT8**/Cu^{2+} decreased the emission signal. The emission output (emission recovery or emission quenching) of the **ZnPorT8**/M^{2+} system could thus be easily reversed by complexed transition metal (mercury(II) vs. copper(II)) yielding tunable optical probe with excellent selectivity and sensitivity for Cys and GSH (Figure 4). Importantly, absorption signal of the **ZnPorT8**/M^{2+} supramolecular system is also sensitive to the addition of biothiols. Addition of L-Cys and GSH to the **ZnPorT8**/Hg^{2+} system caused a hyperchromicity and a blue shift of the Soret band, their addition to **ZnPorT8**/Cu^{2+} gave rise to hypochromicity and a red shift. Both emission and absorption signals can thus be used for sensing of Cys and GSH resulting in a dual optical probe with switchable spectroscopic outcome.

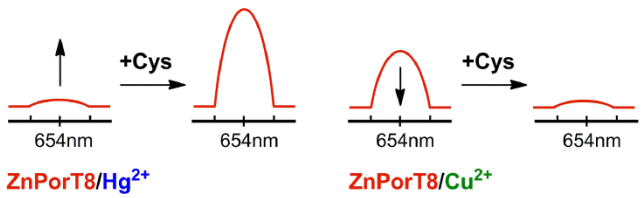

Figure 4. Schematic representation of transition metal induced switch of fluorescence response of **ZnPorT8/Hg(II)** and **ZnPorT8/Cu(II)** supramolecular systems to Cys and GSH.

ZnPorT8/Hg^{2+} and ZnPorT8/Cu^{2+}: Sensitivity of L-Cys and GSH detection using emission signals

To evaluate the sensitivity of the **ZnPorT8**/Hg^{2+} probe, we performed UV-vis absorption and fluorescence titration by adding L-Cys or GSH (1.0 μM - 10.0 μM) to the **ZnPorT8**/Hg^{2+} solution ([**ZnPorT8**] = 2.0 μM, [Hg^{2+}] = 5.0 μM). Figure 5 shows the fluorescence titration of the L-Cys to **ZnPorT8**/Hg^{2+}. The fluorescence intensity gradually increased with increasing concentration of the L-Cys and reached a plateau at [L-Cys] = 5.0 μM. We observed a linear correlation of fluorescence intensity at 654 nm as a function of the L-Cys concentration in the range between [L-Cys] = 0 and 5.0 μM with a slope of 136.79 (Figure 5b). The emission limit of detection (LOD(em)) was determined to be [Cys] = 5.95 nM (3σ/slope, σ = 0.27). All detection limits are summarized in Table 1. Similarly to the L-Cys, fluorescence intensity of the **ZnPorT8**/Hg^{2+} system increased with the increasing concentration of the GSH with a plateau at [GSH] ≥ 3.0 μM (Figure 5c). A linear correlation of 654 nm fluorescence signal as a function of the GSH concentration was observed between [GSH] = 0 and 3.0 μM (Figure 5d). The LOD(em) for GSH was determined to be 3.34 nM (3σ/slope, σ = 0.27) with a slope of 243.47 (Figure 5d).

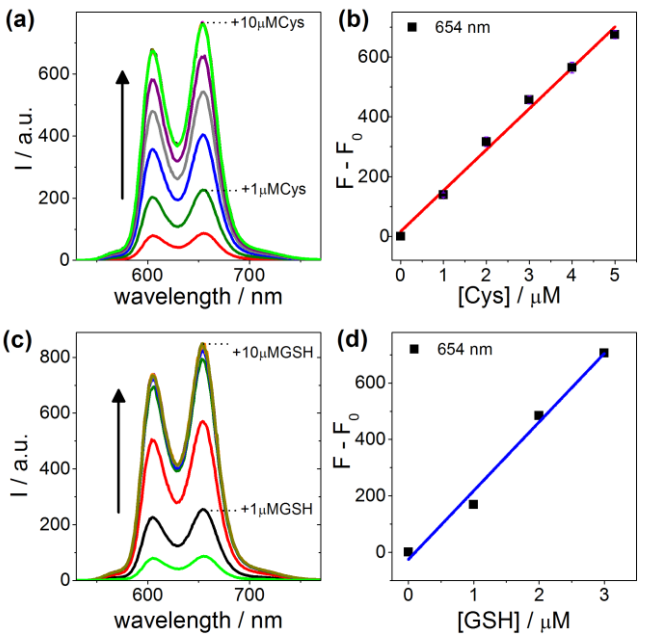

Figure 5. Fluorescence spectra (λ_{exc} = 425 nm) of the (**ZnPorT8**/Hg^{2+} complex ([**ZnPorT8**] = 2.0 μM, [Hg^{2+}] = 5.0 μM) titrated with (a) L-Cys [L-Cys] = 1.0 μM to 10.0 μM in 1.0 μM addition steps) or (c) with GSH ([GSH] = 1.0 μM to 10.0 μM in 1.0 μM addition step). F-F_0 fluorescence intensity changes of the **ZnPorT8**/Hg^{2+} systems as a function of the (b) L-Cys or (d) GSH concentration (0 to 5.0 μM, black squares) detected at 654.0 nm and their linear fits (F-F_0, F_0: fluorescence intensity of **ZnPorT8**/Hg^{2+}, F: fluorescence intensity **ZnPorT8**/Hg^{2+} after addition of biothiols). Arrows depict the biothiol induced changes of the **ZnPorT8**/Cu^{2+} spectroscopic signal.

Stepwise addition of L-Cys (from 1.0 to 6.0 μM in 1.0 μM increments) to the **ZnPorT8**/Cu^{2+} system ([**ZnPorT8**] = 2.0 μM, [Cu^{2+}] = 20.0 μM) caused a decrease of the fluorescence intensity at 654.0 nm by 79.9 % (from 401 a.u. to 80 a.u.; Figure 6a). A linear correlation of the 654.0 nm fluorescence signal as a function of concentration yielded LOD(em) for L-Cys of 11.99 nM (3σ/slope, σ = 0.3823, slope = 95.65, Figure 6b). All detection limits are summarized in Table 1. Similarly, incremental addition of GSH (from 1.0 to 6.0 μM in 1.0 μM steps) induced quenching of fluorescence of **ZnPorT8**/Cu^{2+}. The emission signal at 654 nm dropped by 80.3% (from 400 a.u. to 79 a.u.; Figure 6c) yielding excellent sensitivity for the detection of GSH with $LOD(em)_{GSH}$ = 13.50 nM (3σ/slope, σ = 0.3823, slope = 84.93, Figure 6d).

ZnPorT8/Hg^{2+} and ZnPorT8/Cu^{2+}: Sensitivity of L-Cys and GSH detection using VIS absorption signals

Since the addition of Cys or GSH also caused significant changes in the UV-vis absorption spectra of **ZnPorT8**/Hg^{2+} and **ZnPorT8**/Cu^{2+} systems, we have explored the possibility to sense biological thiols by VIS absorption spectroscopy.

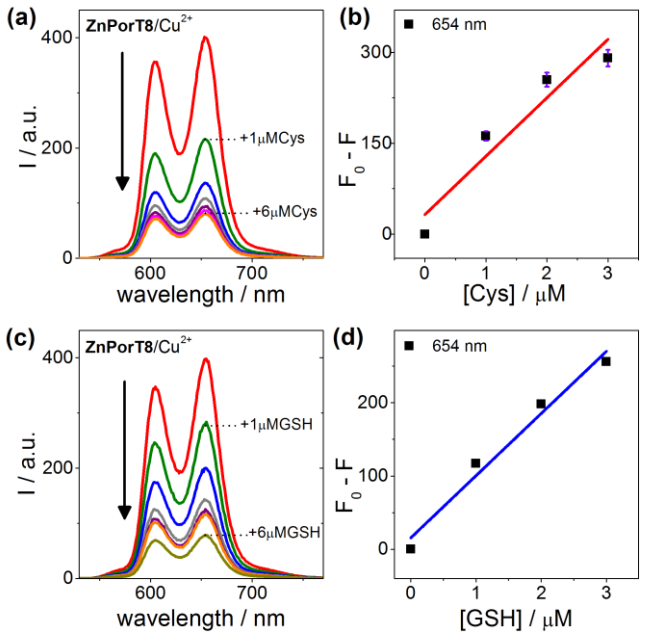

Figure 6. Fluorescence spectra (λ_{exc} = 425 nm) of the (**ZnPorT8**/Hg^{2+} complex ([**ZnPorT8**] = 2.0 μM, [Cu^{2+}] = 20.0 μM) titrated with (a) L-Cys [L-Cys] = 1.0 μM to 6.0 μM in 1.0 μM addition steps) or (c) with GSH ([GSH] = 1.0 μM to 6.0 μM in 1.0 μM addition step). F-F_0 fluorescence intensity changes of the **ZnPorT8**/Cu^{2+} systems as a function of the (b) L-Cys or (d) GSH concentrations (0 to 3.0 μM, black squares) detected at 654.0 nm and their linear fits (F_0-F, F_0: fluorescence intensity of **ZnPorT8**/Cu^{2+}, F: fluorescence intensity **ZnPorT8**/Cu^{2+} after addition of biothiols). Arrows depict the biothiol induced changes of the **ZnPorT8**/Cu^{2+} spectroscopic signal.

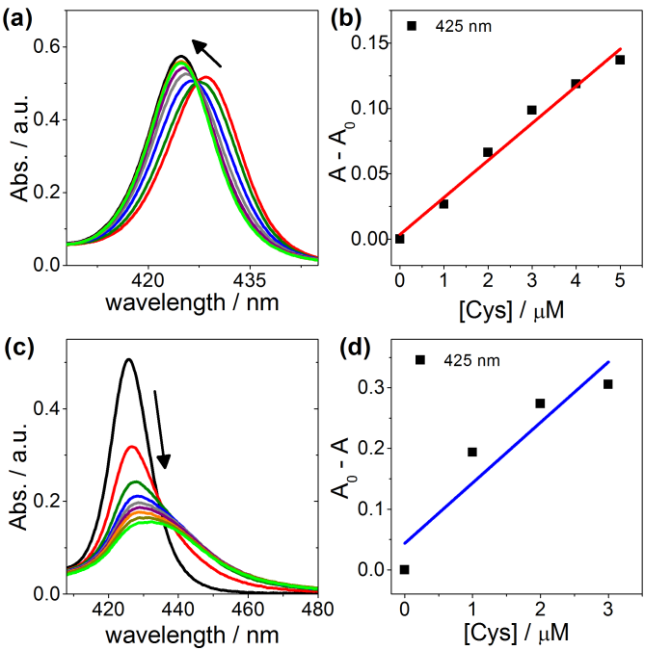

Figure 7. UV-vis absorption spectra (Soret band) of the (a) **ZnPorT8**/Hg^{2+} complex ([**ZnPorT8**] = 2.0 μM, [Hg^{2+}] = 5.0 μM) and (c) **ZnPorT8**/Cu^{2+} complex ([**ZnPorT8**] = 2.0 μM, [Cu^{2+}] = 20.0 μM) titrated with L-Cys [L-Cys] = 1.0 μM to 10.0 μM in 1.0 μM addition steps). A-A_0 absorbance intensity changes of the (b) **ZnPorT8**/Hg^{2+} and (d) **ZnPorT8**/Cu^{2+} systems as a function of the L-Cys concentration (0 to 5.0 μM and 0 to 3.0 μM; black squares) detected at 425.0 nm and their linear fit (A-A_0, A_0: absorbance of **ZnPorT8**/Hg^{2+} or **ZnPorT8**/Cu^{2+}, A: absorbance **ZnPorT8**/Hg^{2+} or **ZnPorT8**/Cu^{2+} after addition of L-Cys). Arrows depict the biothiol induced changes of the **ZnPorT8**/Cu^{2+} spectroscopic signal.

ZnPorT8/Hg^{2+} complex showed a blue shift of the Soret band from 428.6 nm to 425.0 nm with an isosbestic point at 427.0 nm upon stepwise addition of Cys (Figure 7). A linear response of the absorption intensity at 425.0 nm as a function of the L-Cys ([L-Cys] = 0 and 5.0 μM) concentration was observed. The $LOD(abs)_{Cys}$ was calculated to be 531 nM (3σ/slope, σ = 0.005, slope = 0.028, Figure 7b). On the other hand, stepwise addition of Cys to **ZnPorT8**/Cu^{2+} system caused a red shift of the Soret band accompanied by hypochromicity (Figure 7c). A linear response of the absorption intensity at 425.0 nm as a function of the L-Cys ([L-Cys] = 0 and 3.0 μM) yielded $LOD(abs)_{Cys}$ of 531 nM (3σ/slope, σ = 0.005, slope = 0.028, Figure 7d). The GSH LOD(abs) are summarized in Table 1. The absorption data confirmed that **ZnPorT8**/M^{2+} systems (M^{2+} = Hg^{2+} or Cu^{2+}) can be used as dual optical probes for emission as well as absorption biomolecular recognition of biothiols. Lower emission LOD(em) in comparison to absorption LOD(abs) of **ZnPorT8**/M^{2+} systems originated from a larger change of emission signal that positively benefited from Cys- and GSH-induced change of absorbance signal at excitation wavelength (425.0 nm). All LODs are summarized in Table 1.

Table 1. Emission and absorption detection limits of L-Cys and GSH

amino acid [a]	LOD	**ZnPorT8**/Hg^{2+} [a]	**ZnPorT8**/Cu^{2+} [b]
L-Cys	LOD(em)	5.95 nM (enhancement)	11.99 nM (quenching)
	LOD(abs)	531 nM	263 nM
GSH	LOD(em)	3.34 nM (enhancement)	13.50 nM (quenching)
	LOD(abs)	511 nM	256 nM

[a] [**ZnPorT8**] = 2.0 μM, [Hg^{2+}] = 5.0 μM; sodium cacodylate buffer (1 mM, pH 7.0). [b] [**ZnPorT8**] = 2.0 μM, [Cu^{2+}] = 20.0 μM; sodium cacodylate buffer (1 mM, pH 7.0).

We have also examined the effect of concentration of Hg^{2+} in **ZnPorT8**/Hg^{2+} system on fluorescence cysteine detection limits ($LOD(em)_{Cys}$). Figure S30 shows the fluorescence intensity changes detected at 654.0 nm of **ZnPorT8**/Hg^{2+} system ([**ZnPorT8**] = 2.0 μM) with five different concentrations of the Hg^{2+} ion (2.0, 3.0, 4.0, 5.0, and 6.0 μM) upon titration with Cys ([Cys] = 1.0 to 10 μM in 1.0 μM addition step). The $LOD(em)_{Cys}$ have been determined to be 5.16 nM ([Hg^{2+}] = 2.0 μM), 4.48 nM ([Hg^{2+}] = 3.0 μM), 5.51 nM ([Hg^{2+}] = 4.0 μM), 5.95 nM ([Hg^{2+}] = 5.0 μM), and 6.39 nM ([Hg^{2+}] = 6.0 μM) (Figure 10b). The concentration of Hg^{2+} in **ZnPorT8**/Hg^{2+} system showed a clear potential to further

tune the sensitivity of the supramolecular system towards biothiols.

ZnPorT8/Hg^{2+}: Selectivity of L-Cys and GSH detection

To evaluate the selectivity of **ZnPorT8**/Hg^{2+} complex for the spectroscopic detection of biothiols, the UV-vis absorption and emission spectroscopic changes were investigated with 17 other amino acids, i.e. Ala, Arg, Asn, Gln, Glu, Gly, His, Ile, Leu, Lys, Met, Pro, Phe, Ser, Thr, Tyr, and Trp. Figure 8 illustrates the fluorescence response of **ZnPorT8**/Hg^{2+} complex at 654 nm (λ_{ex} = 425 nm) upon addition of different amino acids. UV-vis absorption and fluorescence spectra of the **ZnPorT8**/Hg^{2+} complex ([**ZnPorT8**] = 2.0 μM, [Hg^{2+}] = 5.0 μM) showed very little changes upon the addition of any of these 17 amino acids, even at higher concentrations (up to 30 μM, Figures S8-25). Although the Hg^{2+} ion is known to bind to *N*-heterocycles, our data indicated that the Hg^{2+} affinity for **ZnPorT8** is greater than for tested *N*-heterocyclic amino acids (i.e. Thr, His). **ZnPorT8**/Hg^{2+} system exhibited excellent sensitivity for L-Cys and GSH over other amino acids.

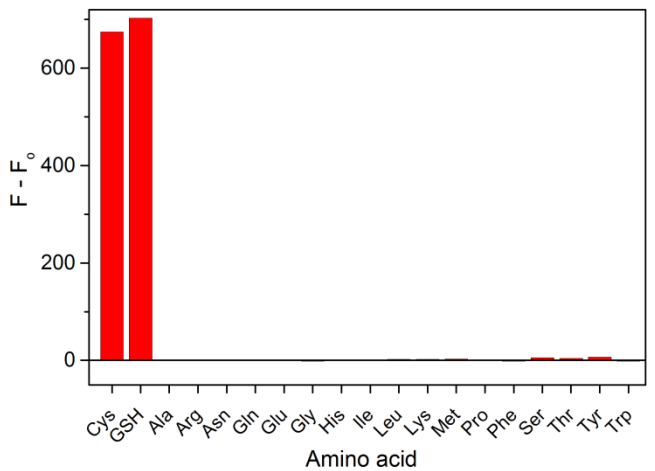

Figure 8. Fluorescence intensity changes of solution of the **ZnPorT8**/Hg^{2+} complex ([**ZnPorT8**] = 2.0 μM, [Hg^{2+}] = 5.0 μM) at 654.0 nm upon addition of amino acids ([Cys] = 5.0 μM, [GSH] = 5.0 μM, [other amino acids] = 10.0 μM).

Next, we evaluated the performance of the **ZnPorT8**/Hg^{2+} system under conditions in which several analytes were present at high concentrations (competition experiments). We prepared a mixture of amino acids containing Ala, Lys, Met, Pro and Trp, and we also made another mixture of the same amino acids that also contained L-Cys. The concentration of each amino acid was set to 5.0 μM (total amino acid concentrations were 30.0 μM and 25.0 μM, respectively). We added aliquots of these amino acid mixtures to the **ZnPorT8**/Hg^{2+} complex ([**ZnPorT8**] = 2.0 μM, [Hg^{2+}] = 5.0 μM) and recorded absorption and fluorescence spectroscopic changes (ESI, Figure S31). Addition of the amino acid mixture without L-Cys did not show any evident spectroscopic changes. On the other hand, the mixture containing L-Cys caused very similar spectroscopic changes to neat L-Cys: the blue shift of the Soret absorption band from 430.0 to 425.0 nm and an increase of the fluorescence signal recorded at 654 nm (λ_{ex} = 425.0 nm). The results of the competition experiments confirmed that non-thiol amino acids did not interfere with L-Cys sensing by using the absorption and emission spectroscopic responses of the **ZnPorT8**/Hg^{2+} complex.

Experimental

Materials

Amino acids (L-Cys, D-Cys, L-GSH, Ala, Arg, Asn, Gln, Gly, Glu, His, Ile, Leu, Lys, Met, Pro, Phe, Ser, Thr, Tyr, Trp, and Val), $Hg(ClO_4)_2$, $Cu(ClO_4)_2$, and sodium cacodylate were purchased from Sigma-Aldrich. Ultrapure water was obtained from a Milli-Q system with a resistivity of 18.2 MΩ·cm. Synthesis, purification and characterization of zinc(II)porphyrin-oligothymine conjugate **ZnPorT8** has been reported previously.[53, 54]

Methods

The stock solutions of **ZnPorT8**, Hg^{2+}, Cu^{2+}, and all amino acids were prepared in a sodium cacodylate buffer (1 mM, pH 7.0). The concentration of **ZnPorT8** stock solution was determined by UV-vis absorption spectroscopy using the extinction coefficient $\varepsilon_{\mathbf{ZnPorT8}} = 2.9 \times 10^5\ M^{-1}\ cm^{-1}$ at 425 nm.[53, 54] The fluorescence and absorption titration experiments were performed as follows: aliquots of amino acids (0.8 μL, concentration of the stock solutions = 1 mM) were added into a 800 μL solution of the **ZnPorT8**/M^{2+} complex (M^{2+} = Hg^{2+} or Cu^{2+}, [**ZnPorT8**] = 2.0 μM, [Hg^{2+}] = 5.0 μM, [Cu^{2+}] = 20.0 μM) in the sodium cacodylate buffer (1 mM, pH = 7.0). The absorption and emission spectra were recorded upon each addition. The collected spectroscopic data have been corrected for dilution (in all cases dilution was kept below 1%).

Instrumentation

UV-vis absorption spectra were collected at 20 ºC using a Jasco V-650 UV-vis double beam spectrophotometer equipped with a single position Peltier temperature control system. Fluorescence measurements were performed at 20 ºC on a Varian Cary Eclipse fluorescence spectrophotometer equipped with a Peltier temperature control system. The emission spectra were collected from 500 to 800 nm with an excitation wavelength of 425.0 nm. Conditions were as follows: excitation slit 10 nm, emission slit 10 nm, scan rate 600 nm/min. A quartz cuvette with a 1 cm path length was used for all absorption and emission experiments.

Conclusions

We have reported a tunable supramolecular system assembled from the zinc(II)porphyrin-oligothymidine conjugate (**ZnPorT8**) and a transition metal ion as a dual (emission/absorption) highly selective and sensitive optical probe for biothiol. We have shown that the fluorescence as well as absorption response of **ZnPorT8** can be switched by a complexed metal ion (either Hg(II) or Cu(II)). The **ZnPorT8**/Hg^{2+} complex offered a turn-on fluorescence sensing

of Cys and GSH (fluorescence enhancement), while the **ZnPorT8**/Cu^{2+} system exhibited reversed turn-off sensing (fluorescence quenching). Both turn-on as well as turn-off biomolecular optical detection can be achieved using the same bioorganic scaffold. Importantly, while the transition metal ions modulated the optical outcome, they had only marginal effect on the sensitivity of the **ZnPorT8**/M^{2+} supramolecular system. Both complexes (**ZnPorT8**/Hg^{2+} and **ZnPorT8**/Cu^{2+}) displayed excellent limit of detection using emission signal for Cys (LOD(em) = 5.95 nM and 11.99 nM, respectively) and GSH (LOD(em)= 3.34 nM and 13.50 nM, respectively) using the 3σ/slope method. The other 17 proteinogenic amino acids did not cause any significant fluorescence or absorption signal changes when added to **ZnPorT8**/Hg^{2+}.

Acknowledgements

We thank UW SER Graduate Assistantship (GS), Center for Photoconversion and Catalysis, Department of Chemistry Graduate Assistantship (JKC) and Wyoming INBRE undergraduate research fellowship (BDJ). We thank Prof. Ed Clennan (Department of Chemistry, UW) for acquisition of and access to the Varian Cary Eclipse fluorescence spectrophotometer.

Notes and references

[a] Department of Chemistry, University of Wyoming, 1000 E. University Avenue, Laramie, WY 82071, USA.

† Electronic Supplementary Information (ESI) available: UV-vis absorption and emission spectra of **ZnPorT8**/Hg^{2+} and **ZnPorT8**/Cu^{2+} complexes titrated with different amino acids. See DOI: 10.1039/b000000x/

1. M. Biesaga, K. Pyrzynska and M. Trojanowicz, *Talanta*, 2000, **51**, 209-224.
2. Z. J. Li and J. M. Pan, *Rev. Anal. Chem.*, 2002, **21**, 167-231.
3. L. Lvova, C. Di Natale and R. Paolesse, *Sensor Actuat B: Chem*, 2013, **179**, 21-31.
4. T. Kerdcharoen and S. Kladsomboon, in *Applications of Nanomaterials in Sensors and Diagnostics*, ed. A. Tuantranont, Springer Berlin Heidelberg, 2013, pp. 237-255.
5. D. Papkovsky and T. O'Riordan, *J. Fluoresc.*, 2005, **15**, 569-584.
6. R. Purrello, S. Gurrieri and R. Lauceri, *Coord. Chem. Rev.*, 1999, **190–192**, 683-706.
7. M. K. Kuimova, S. W. Botchway, A. W. Parker, M. Balaz, H. A. Collins, H. L. Anderson, K. Suhling and P. R. Ogilby, *Nat. Chem.*, 2009, **1**, 69-73.
8. L. P. Jameson, J. D. Kimball, Z. Gryczynski, M. Balaz and S. V. Dzyuba, *RSC Adv.*, 2013, **3**, 18300-18304.
9. C. X. Guo, Y. Lei and C. M. Li, *Electroanalysis*, 2011, **23**, 885-893.
10. J. K. Choi, A. D'Urso and M. Balaz, *J. Inorg. Biochem.*, 2013, **127**, 1-6.
11. A. E. Holmes, J. K. Choi, J. Francis, A. D'Urso and M. Balaz, *J. Inorg. Biochem.*, 2012, **110**, 18-20.
12. J. K. Choi, G. Sargsyan, M. Shabbir-Hussain, A. E. Holmes and M. Balaz, *J. Phys. Chem. B*, 2011, **115**, 10182-10188.
13. J. K. Choi, A. Reed and M. Balaz, *Dalton Trans.*, 2014, **43**, 563-567.
14. X. D. Wang and O. S. Wolfbeis, *Chem. Soc. Rev.*, 2014, **43**, 3666-3761.
15. E. Bellacchio, R. Lauceri, A. Magri, R. Purrello, S. Gurrieri, L. Monsu Scolaro and A. Romeo, *Chem. Commun.*, 1998, 1333-1334.
16. X.-H. Li, Z.-H. Xie, H. Min, Y.-Z. Xian and L.-T. Jin, *Electroanalysis*, 2007, **19**, 2551-2557.
17. B. J. White and H. J. Harmon, *IEEE Sensors J.*, 2005, **5**, 726-732.
18. J. K. Choi, G. Sargsyan, A. M. Olive and M. Balaz, *Chem. Eur. J.*, 2013, **19**, 2515-2522.
19. A. Rigo, A. Corazza, M. Luisa di Paolo, M. Rossetto, R. Ugolini and M. Scarpa, *J. Inorg. Biochem.*, 2004, **98**, 1495-1501.
20. I. Onyido, A. R. Norris and E. Buncel, *Chem. Rev.*, 2004, **104**, 5911-5930.
21. K.-H. Leung, H.-Z. He, V. P.-Y. Ma, D. S.-H. Chan, C.-H. Leung and D.-L. Ma, *Chem. Commun.*, 2013, **49**, 771-773.
22. H. Xu, Y. Wang, X. Huang, Y. Li, H. Zhang and X. Zhong, *Analyst*, 2012, **137**, 924-931.
23. K. S. Park, M. I. Kim, M.-A. Woo and H. G. Park, *Biosens. Bioelectron.*, 2013, **45**, 65-69.
24. A. K. Mahapatra, J. Roy, P. Sahoo, S. K. Mukhopadhyay, A. Banik and D. Mandal, *Tetrahedron Lett.*, 2013, **54**, 2946-2951.
25. Q. Lin, Y. Huang, J. Fan, R. Wang and N. Fu, *Talanta*, 2013, **114**, 66-72.
26. H. Xu and M. Hepel, *Anal. Chem.*, 2011, **83**, 813-819.
27. B. Han, J. Yuan and E. Wang, *Anal. Chem.*, 2009, **81**, 5569-5573.
28. N. Kaur, P. Kaur and K. Singh, *RSC Adv.*, 2014, **4**, 29340-29343.
29. X. Jia, J. Li and E. Wang, *Chem. Eur. J.*, 2012, **18**, 13494-13500.
30. Y. Gao, Y. Li, X. Zou, H. Huang and X. Su, *Anal. Chim. Acta*, 2012, **731**, 68-74.
31. L. Chang, T. Wu and F. Chen, *Microchim. Acta*, 2012, **177**, 295-300.
32. F. Y. Wu, W. S. Liao, Y. M. Wu and X. F. Wan, *Spectrosc. Lett.*, 2008, **41**, 393-398.
33. W. S. Liao, F. Y. Wu, Y. M. Wu and X. J. Wang, *Microchim. Acta*, 2008, **162**, 147-152.
34. J. Zong, X. Yang, A. Trinchi, S. Hardin, I. Cole, Y. Zhu, C. Li, T. Muster and G. Wei, *Biosens. Bioelectron.*, 2014, **51**, 330-335.
35. S. Shahrokhian, *Anal. Chem.*, 2001, **73**, 5972-5978.
36. Y. Zhang, Y. Li and X.-P. Yan, *Anal. Chem.*, 2009, **81**, 5001-5007.
37. B. Han, J. Yuan and E. Wang, *Anal. Chem.*, 2009, **81**, 5569-5573.
38. A. Chauhan and V. Chauhan, *Pathophysiology*, 2006, **13**, 171-181.
39. S. M. Deneke, *Curr. Top. Cell. Regul.*, 2000, **36**, 151-180.
40. X. F. Wang and M. S. Cynader, *J. Neurosci*, 2001, **21**, 3322-3331.
41. S. Seshadri, A. Beiser, J. Selhub, P. F. Jacques, I. H. Rosenberg, R. B. D'Agostino, P. W. F. Wilson and P. A. Wolf, *Eng. J. Med.*, 2002, **346**, 476-483.
42. A. Meister, *Science*, 1983, **220**, 472-477.
43. N. Burford, M. D. Eelman, D. E. Mahony and M. Morash, *Chem. Comm.*, 2003, 146-147.
44. A. Levina and P. A. Lay, *Inorg. Chem.*, 2003, **43**, 324-335.
45. Y. Zhou and J. Yoon, *Chem. Soc. Rev.*, 2012, **41**, 52-67.
46. X. Dai, Q.-H. Wu, P.-C. Wang, J. Tian, Y. Xu, S.-Q. Wang, J.-Y. Miao and B.-X. Zhao, *Biosens. Bioelectron.*, 2014, **59**, 35-39.
47. J. Zhu, X. Song, L. Gao, Z. Li, Z. Liu, S. Ding, S. Zou and Y. He, *Biosens. Bioelectron.*, 2014, **53**, 71-75.
48. W. Stricks and I. M. Kolthoff, *J. Am. Chem. Soc.*, 1953, **75**, 5673-5681.

49. Kevin K. Divine, F. Ayala-Fierro, D. S. Barber and D. E. Carter, *J. Toxicol. Environ. Health, Part A*, 1999, **57**, 489-505.
50. L. Pecci, G. Montefoschi, G. Musci and D. Cavallini, *Amino Acids*, 1997, **13**, 355-367.
51. T. Wen, S. Hou, J. Yan, H. Zhang, W. Liu, Y. Ji and X. Wu, *RSC Adv.*, 2014, **4**, 45159-45162.
52. J. H. Freedman, M. R. Ciriolo and J. Peisach, *J. Biol. Chem.*, 1989, **264**, 5598-5605.
53. G. Sargsyan and M. Balaz, *Org. Biomol. Chem.*, 2012, **10**, 5533-5540.
54. G. Sargsyan, B. L. MacLeod, U. Tohgha and M. Balaz, *Tetrahedron*, 2012, **68**, 2093–2099.